Available online at www.sciencedirect.com
SCIENCE DIRECT
Journal of Physics and Chemistry of Solids 67 (2006) 690–697
JOURNAL OF PHYSICS AND CHEMISTRY OF SOLIDS
www.elsevier.com/locate/jpcs

Adhesion and bonding of Pt/Ni and Pt/Co overlayers: Density functional calculations

Gabriela F. Cabeza [a], Norberto J. Castellani [a,*], Pierre Légaré [b]

[a] Departamento de Física, Universidad Nacional del Sur, Avda. Alem 1253, Bahía Blanca B8000CPB, Argentina
[b] LMSPC. Groupe Surfaces et Modélisation, ECPM. 25 rue Becquerel, F-67087 Strasbourg Cedex 2, France

Received 19 May 2005; received in revised form 30 August 2005; accepted 4 October 2005

Abstract

The electronic and energetic properties of bimetallic surfaces Pt/Ni(111) and Pt/Co(111) are examined using the FP-LAPW (*Full-Potential Linearized Augmented Plane Wave*) method by means of spin-polarized and non-polarized calculations. We present both the results of the shifts in the d-band centers when one metal (Pt) is pseudomorfically deposited on another with smaller lattice constant (Ni, Co) and those corresponding to the surface and adhesion energies. The surface is modeled by a seven layer slab separated in z direction by a vacuum region of six substrate layers. The results obtained for pure Ni, Co and Pt surfaces are presented in order to compare with experimental and theoretical data reported in the literature

Keywords: A. Surfaces; C. Ab initio calculations; D. Electronic structure

1. Introduction

Recently, the interest to study the reactive properties of alloys and bimetallic surfaces has increased notably taking into account the fact that they can show significant differences with respect to their pure components. Theoretical approaches to this problem have shown that d-valence levels are mainly involved in this behaviour and that when different metals are in tight contact, it is possible to shift the local atomic d-bands, opening a way to adjust the surface of transition metals (TM) in order to be more active in adsorption and surface reactions [1]. In the particular case of Pt on Ni(111) and Co(0001) previous theoretical calculations and experimental results have shown that the strength adsorption of molecules like CO on Pt decreases significantly in comparison with pure Pt [2,3].

The main goal of the present work is to study the structural and electronic properties of group VIII TM bimetallic systems, particularly when Pt is deposited on close packed surfaces of Ni and Co. In the past, we studied these systems employing no spin polarized semiempirical [2–4] and ab initio methods [5].

Here, this phenomenon is analysed on a comparative basis considering the electronic structure of four different systems: the pseudomorfic Pt/Ni(111) and Pt/Co(0001) overlayers, the normal Pt(111) surface and a fictive Pt(111) surface denoted as Pt′(111) where the Pt–Pt interatomic distance is set equal to that of bulk Ni. In this way, we can observe what the chemical effect of replacing the Pt substrate by another metal like Ni or Co is.

In the case of the overlayers, Pt is supposed to be in epitaxis. This hypotesis in the case of low Pt coverages (<2 mL) can be justified from the experimental results reported by several authors. The two metals forming the interfaces present compatible symmetries as Pt and Ni crystallize in the fcc system and Co in the hcp form. However, the big misfit of the crystalline parameters between Pt and Ni (about 11%) or Pt and Co (about 10%) could prevent a layer-by-layer psedomorphic growth. Bauer et al. [6] predicted that beyond a misfit of about 5%, dislocations would take place in the overlayer in order to relax the stress. Note, however, that as Pt has the bigger crystalline parameter, the overlayer should be submitted to compression, which can favor our model. Furthermore, a similar or even higher misfit does not seem to prevent a layer-by-layer growth, as it is demonstrated by the literature of the subject [7].

Recently, we published the results obtained by a numerical simulation of growth of pseudomorphic Pt layers (from 1 to 4) on Ni(111) and Co(0001) [4]. For that purpose, we considered

* Corresponding author. Tel.: +54 291 4595141; fax: +54 291 4595142.
E-mail address: castella@criba.edu.ar (N.J. Castellani).

0022-3697/$ - see front matter © 2005 Elsevier Ltd. All rights reserved.
doi:10.1016/j.jpcs.2005.10.178

the formation of a hypotetical pseudomorphic overlayer. Despite an important compression of the Pt deposit ($\approx 10\%$), it was proved that the one-Pt-layer system was even more stable than the pure bulk substrate. These results were explained considering two factors: (1) the chemical affinity between the two metals in contact and (2) the compression in the surface plane which provides an increased electron density on the platinum sites that balance the lowered density due to the surface broken Pt bonds. On the other hand, the Pt-multilayered systems were less stable because the compression destabilizes the Pt internal planes. These conclusions are compatible with the experimental results obtained on the same systems. On Ni(111) [8,9], platinum grows with a (likely imperfect) layer-by-layer mode, but the ease of formation of surface alloys with a moderate temperature increase favors the metastable character of multilayers films and confirms the chemical affinity between the two metals. The picture looks similar for Pt/Co(0001) [10], although some interdiffusion of the metals was reported [11]. Therefore, we assume in the present study that the Pt film adopts the substrate parameter.

The organization of this work is as follows. In a first section we give a brief description of the theoretical method and the model employed. Afterward, a section is devoted to analyze the electronic properties of the systems; the density of states curves were used to obtain the d-band shifts of surface pseudomorphic overlayers relative to the clean Pt metal. In addition, a comparative study employing spin polarized calculations was performed, particularly to analyze the local magnetism of such bimetallic systems. We end showing the results obtained for adhesion and surface energies and making the comparison with experimental data and other theoretical calculations.

2. Calculational details

The calculations were performed using Density Functional Theory (DFT). The exchange-correlation functional was treated according to the Generalized-Gradient Approximation (GGA) in the parameterization of PBE [12]. The corresponding Kohn-Sham equations were solved applying the *Full-potential Linearized Augmented Plane-wave* (FP-LAPW) method. The (111) surface was simulated by periodically repeated slabs of seven layers separated in z-direction by a vacuum region (Fig. 1). The width of this gap was optimized to avoid the interaction between slabs. For that purpose, we observed that a distance of six atomic layers was sufficient. We noticed also that a gap corresponding to four substrate layers did not show important differences for all systems except for Pt; in this case an excess of charge at surface atoms was observed.

For the pure Pt, Ni and Co models, the nearest Pt–Pt, Ni–Ni and Co–Co distances were set to 2.807 [5], 2.489 [2] and 2.510 Å [5], respectively, whereas for Pt/Ni and Pt/Co, Ni and Co atoms of the first layers were substituted by Pt atoms, respectively. The distances between surface and subsurface planes for the bimetallic surfaces were adjusted employing their atomic radii. The other planes were maintained at their respective bulk positions (Ni, Co).

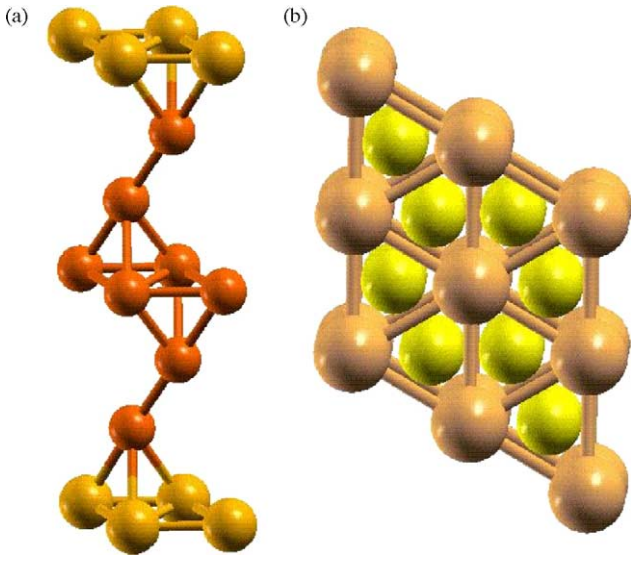

Fig. 1. (a) Ball and sticks view of the bimetallic unit cell. There are 7 atoms by unit cell (4 no equivalent by symmetry). Pt, large spheres; Ni or Co, small spheres. (b) A packing drawing corresponding to the projection of the unit cell showed in (a).

The Co was modellized employing a fcc structure in order to facilitate the comparison between systems. The Co crystallizes into hcp structure below 950 K; nevertheless, the fcc phase becomes experimentally stable with a swift quenching.

The bulk energy systems were calculated considering the [111] direction to compare with the (111) surfaces. In order to prevent overlap of the MT spheres, the muffin-tin radius (R_{MT}) was fixed at 2.35 bohr for Ni and Co. In the case of Pt the R_{MT} was 2.60 bohr. The LAPW wave functions within the muffin-tins were expanded in spherical harmonics with angular momenta up to lmax = 10 and plane waves up to an energy cutoff of $|K_{max}|^2 = 14.7$ Ry are employed. The (l,m) expansion for the potential goes up to lmax = 4. The cutoff energy for the Fourier-series expansions of the interstitial electron density and potential was $|G_{max}|^2 = 169$ Ry. The Brillouin zone integration was made using 52 k points. In order to take into account the magnetic properties of Co and Ni, the computations were performed at the spin-polarized level (sp). To compare with other results reported in the literature and obtained with different methods, non-polarized (nsp) calculations were also presented.

3. Results and discussion

3.1. Electronic properties

The interest in analizing the bimetallic substrates in gas/solid interfaces is twofold: (i), to show their influence in the adsorption of gases; in previous theoretical results of similar systems [3], we noticed a decrease of the magnitude of adsorption energy in comparison with pure metals, and (ii), to know if this change corresponds to a chemical, a geometrical or both effects. In order to test the geometrical influence, an

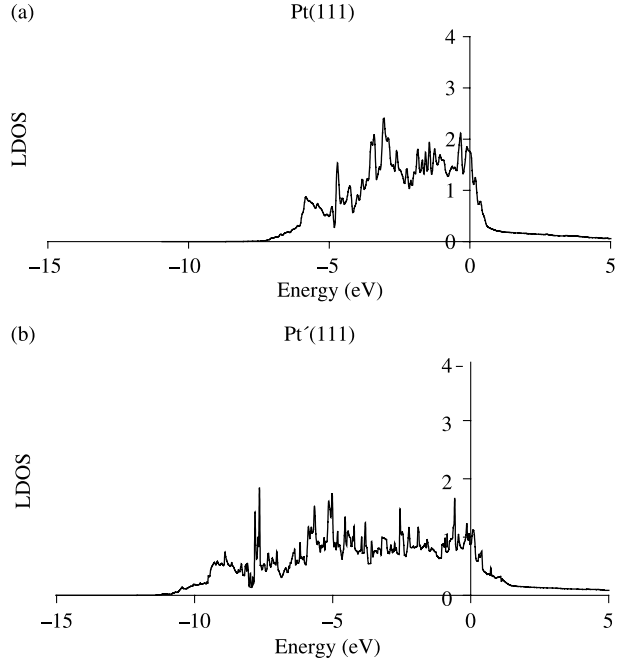

Fig. 2. Local density of states (LDOS) of the d-band of the adsorbate layer (Pt) obtained from a non-magnetic calculation. The origin of the energy scale corresponds to the Fermi level. (2a) Pt(111) surface; (2b) Pt′(111) surface. Artificial Pt crystalline structure (noted Pt′) with a Pt–Pt interatomic distance of 2.489 Å (equal to that of Ni bulk).

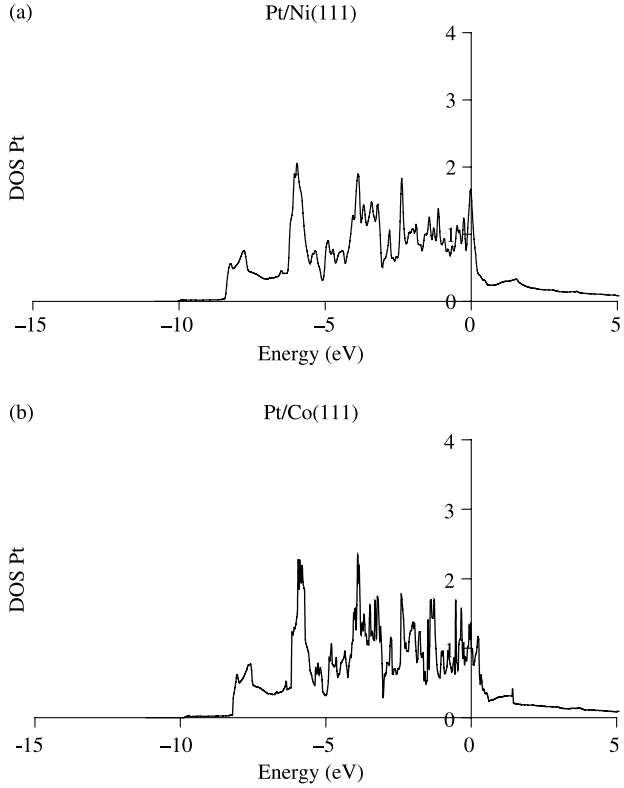

Fig. 3. Local density of states (LDOS) of the d-band of the adsorbate layer (Pt) obtained from a non-magnetic calculation. The origin of the energy scale corresponds to the Fermi level. (3a) Pt/Ni(111) surface. (3b) Pt/Co(111) surface.

artificial Pt crystalline structure (denoted as Pt′) with a Pt–Pt interatomic distance of Ni bulk (11% lower than that of Pt) was considered.

Let us first comment the results corresponding to Pt electronic structure. In Fig. 2, we present the LDOS curves for the 5d-band of Pt surface (2a) and Pt contracted, Pt′ (2b), both corresponding to the local electronic structure for the Pt surface layer. The principal feature to arise in Fig. 2b is the extension of the Pt-d band down to −11 eV whereas it does not extend below −7 eV in Fig. 2a. Moreover, the d-LDOS(E_F) on Pt′(111) is remarkably lower than on Pt(111) (≈2.0 vs 0.76 eV^{-1}, respectively). This valence band broadening is mainly due to the greater overlap between the Pt atoms related to the Pt–Pt distance reduction from pure Pt to Pt′. Therefore, this behavior is essentially due to a geometrical effect.

The electronic structures showed in Fig. 3, correspond to bimetallic systems Pt/Ni(111) (3a) and Pt/Co(111) (3b). The qualitative trends in Fig. 3a and b are identical. We can appreciate particularly the presence the three peaks around −3.5, −5.7 and −7.6 eV. The Pt 5d-band is wider than that of pure metallic Pt surface, extending up to nearly −8.0 eV. Moreover, the formation of Pt-TM (TM=Ni, Co) bonds produces a depletion in the density of Pt 5d states around the Fermi level (0.14 and 0.69 eV^{-1} for PtNi and PtCo, respectively).

The wider 5d-band could be explained by a purely geometrical effect as in the case of Pt′. Nevertheless, the variations in the energy range covered by d-band of the Pt overlayer are a result of: (1) a reduction in the Pt–Pt distance that increases the width of the Pt d-band and (2) changes in the Pt-substrate interactions that shift the centroid of the d-band toward higher binding energy (see next section). The relative importance of both the structural and the chemical effects through the interactions between the two components should be recognized.

In all cases, the LDOS curves corresponding to surface Pt atoms show, when compared with Pt(111) (2a), an enlargement of the same degree as in a previous semiempirical approach [2]. In an earlier work [13] we reported the photoemission results obtained with He II (40.82 eV) light taken at various coverages of Pt on Co(0001). To obtain a better insight of the structure of the Pt valence electronic states, we subtracted the clean Co spectrum for the He II data (Fig. 4a). New Pt-induced states appeared in the vecinity of 1.5 and 4 eV for He I (not shown) and He II, respectively. In order to make a comparison with our present calculations the electronic structures of pure Co(0001) and Pt/Co(0001) slabs using LAPW theory and spin polarized calculations were computed. For that purpose, first the total DOS of slabs of 14 layers separated in z-direction by a vacuum region of six layers was computed. For the bimetallic case the surface layers of Co was substituted by Pt (as above mentioned). Then the difference between the Pt–Co DOS and that of pure Co was performed in order to mimic the photoemission spectra. The results of this procedure are shown in Fig. 4b. We notice that photoemission profiles of

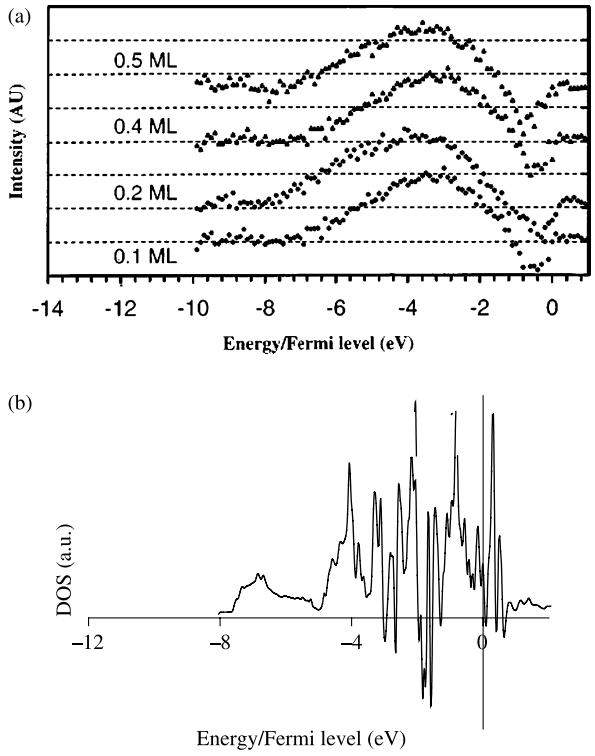

Fig. 4. (a) Left panel. UPS (He II) curves for various Pt deposits obtained in [13] after subtraction of the clean Co contribution (see text). (b) Right panel. Computed curve (up + dn) corresponding to the total DOS of the Pt/Co(0001) slab after subtraction of the pure Co total DOS.

theory and experiment are similar. Fig. 4a and b show a broad feature around −3.5 eV as well as the decrease of DOS below the Fermi level. Examination of the detailed results of the calculations indicates that the states of Pt most affected by the interaction with the substrate are of d character. We can also observe states above Fermi energy. A theoretical treatment analogous to that shown here was performed in the past using semiempirical quantum calculations with metallic clusters [13]. In that approach, we arrived at the same general comparison.

We underline that in Fig. 4b, there exists a broad peak around −7 eV which is absent in Fig. 4a. A possible explanation is that the Pt coverages in UPS spectra are lower to 1 mL. The same peak appears in the computed bulk Pt DOS (not shown here), but shifted to lower BEs by ca 1 eV.

3.2. Calculated variations in d-band centers for pseudomorphic overlayers

The center of the d-band ε_d is an important parameter characterizing the ability of the surface d-electrons to participate in bonding to the adsorbate. The d-band center of a given metal atom will depend on the surroundings, and one of the possibilities for modifying the reactivity of a metal is by depositing it as an overlayer onto the surface layer of another metal. ε_d is defined as the centroid of the d-type density of states in an atomic sphere centered at a surface atom.

Up to present, there are many attempts to correlate catalytic properties; for example, heats of adsorption of molecules (H, CO, ethylene), and the energy of the center of the d-band relative to the Fermi level. In [14] the authors determine whether the trends expected theoretically, employing different calculations methods, are observed experimentally. Hammer and Nørskov [15,16] showed that the heat of adsorption of gases on transition metals (TM) should linearly increase as the energy of the center of the d-band increases, while the heat of adsorption decreases linearly with the strength of the Pauli repulsions. Particularly, for CO adsorption on Pt(111) surface, the slope of the data is about 1/3 of that expected theoretically. Now the question is what the change in the d-band center of a TM (in our case Pt) is when we put it as overlayer onto another metal (Ni, Co) with lower lattice constant.

We report the center of gravity of the d-states obtained starting from the DOS curves presented above (Figs. 2a and 3a and b). For nsp calculations we obtained: −2.61, −3.72 and −3.69 eV for Pt, Pt/Ni and Pt/Co, respectively. For sp calculations the average between up and down values are: −2.62, −3.69 and −3.71 eV in the same order. In a recent work [17], DFT calculations (sp) using the CASTEP code were performed to study the CO adsorption on a Pt/Co surface. The center of gravity of the d-states obtained for Pt and Pt/Co surfaces were at −2.11 and −3.26 eV, respectively. For those calculations the surface structure was relaxed obtaning a Co–Pt interplane distance of 2.287 Å. The width of the Pt d-bands for Pt and Pt/Co are very similar employing both methods: nearly 6 eV for Pt and 8 eV for Pt/Co.

Table 1 summarizes the shifts in d-band centers of surface pseudomorphic overlayers relative to the clean Pt metal (i.e. $\varepsilon_{d,overlayer} - \varepsilon_{d,bulkPt}$) for sp and nsp calculations. The kind of calculation for the overlayer atom (Pt) is listed horizontally and the substrates are listed vertically. In the spin polarized calculations we took the average between the d-band centers obtained for up and down cases. There are not large differences between nsp and sp results (<1%). The inclusion of relaxations decreases the shifts seen in Table 1, but this does not change the sign or relative magnitude of the effect. These observations are in agreement with the tendency presented by Ruban et al. [18]. These authors reported LDA-DFT calculations using the LMTO-ASA method for the surface

Table 1
Shifts in d-band centers of surface pseudomorphic overlayers relative to the clean Pt metal (i.e. εd overlayer – εd bulk Pt) for sp and nsp cases. All values are in eV. The type of calculation for the overlayer atom is listed horizontally and the host entries are listed vertically.

Overlayer →	Pt	
Substrate ↓	nsp	sp (average)
Co	−0.519	−0.576
Ni	−0.547	−0.544
Pt	+0.561	−0.547
Pt′	−1.137	−1.128

electronic structure of pseudomorfic overlayers and impurities of one TM over other TM. The variations in d-band centers were computed for unrelaxed, pseudomorfic overlayers and surface impurities. The systems were modelled with six layers of atomic spheres and two layers of the vacuum spheres. Particularly, they reported the calculated d-band centers of the most close packed surface of the Co, Ni, Pt, Pt/Co and Pt/Ni systems. The value obtained for pure Pt was −2.25 eV. The shifts were −1.89 eV for Pt/Co and −1.53 for Pt/Ni. These results are in the same direction as ours. The Pt-substrate interaction shifts the centroid of the Pt pure d-band toward higher binding energies. The position of d-states with respect to HOMO and LUMO of adsorbing molecule is an important parameter to define the ability of metallic atoms to form a chemical bond with this molecule. Therefore, we verify the existence of a correlation between d-band postion and chemisorption strength. As the d-band of Pt is placed far away from molecular HOMO and/or LUMO, this strength decreases. This is the case for CO adsorbed on Pt/Co and Pt/Ni. Indeed, according to our observations presented in previous works [2,3,17,19,20] and in the literature [21], CO adsorbs much strongly on Pt(111) pure than on a monolayer of Pt on Ni(111) and Co(0001). A decrease in the CO adsorption energy has also been observed for the Pt/Ta, Pt/Zn, Pt/W and Pt/Mo systems (see Fig. 34 of Ref. [22]).

In Table 1, the variations obtained for Pt and Pt′ are also reported. In the first case, the shift of surface Pt with respect to bulk Pt is positive. This is a well-known effect. For a surface atom the neutral radius is larger than in the bulk because the contribution to the electron density around a surface atom from the neighbors is smaller than in the bulk. Consequently, the Pt d-band center at the surface is higher in energy than for bulk Pt. On the other hand, for Pt′ the shift of the d-band center is toward higher binding energies with respect to bulk Pt. This negative shift must be mainly related to the artificial Pt–Pt distance shortening. When a metal atom with a large lattice constant and the filling of the d-band is greater than 0.5 is put as an overlayer at the surface of a metal with a smaller lattice, the width of the d-band increases and, therefore, the local d-band shifts down in order to preserve the degree of d-band filling. In the bimetallic surfaces, this negative shift is also observed but it is of lower magnitude. Evidently for them an additional chemical interaction is present which could account for this effect (see Fig. 5).

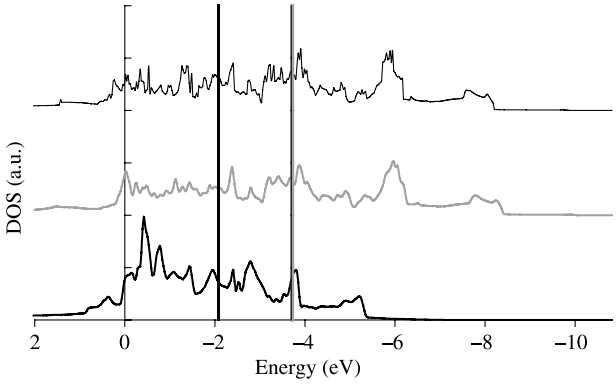

Fig. 5. Local density of states (LDOS) of the Pt d-band of the Pt(111) (lower), PtNi(111) (middle) and PtCo(111) (upper) slabs obtained from a non-magnetic calculation. The origin of the energy scale corresponds to the Fermi level. The vertical lines indicates the d-bands centers of the three systems ($\varepsilon_{dPt111} = -2.612$ eV, $\varepsilon_{dPtNi111} = -3.721$ eV *y* $\varepsilon_{dPtCo111} = -3.693$ eV).

3.3. Energetic properties

3.3.1. Surface and adhesion energy. Work functions

The *surface energy* σ is the energy associated with the creation of a surface. Given the difficulties for the direct measurement of a surface energy, accurate calculations [23] of this quantity play a relevant role in surface science. The standard method for calculating σ is to evaluate the total energy for a slab of the material of interest and then to substract from it the bulk energy obtained in a separate calculation. The *surface energy* σ can be expressed either as an energy per surface atom or per unit surface area:

$$\sigma = \frac{(E^{\text{slab}} - NE^{\text{bulk}})}{2A} \tag{1}$$

where A is the area of the surface unit cell of the considered slab, E^{slab} is the total energy per unit cell of the seven-layer slab, E^{bulk} is the total energy per unit cell of the bulk crystal and N is the number of atoms in the slab supercell (7). The factor 2 accounts for the presence of two surfaces in the slab. For bimetallic systems the surface energy is defined as follows:

$$\sigma_{\text{bim}} = \frac{\left(E^{\text{slab}} - N_{\text{subs}}^{\text{bulk}} E_{\text{subs}}^{\text{bulk}} - N_{\text{sup}}^{\text{bulk}} E_{\text{sup}}^{\text{bulk}}\right)}{2A} \tag{2}$$

where E^{slab} is the total energy per unit cell of the bimetallic slab, $N_{\text{subs}}^{\text{bulk}}$ and $N_{\text{sup}}^{\text{bulk}}$ are the numbers of substrate (5) and surface atoms (2) in the slab, respectively, and finally $E_{\text{subs}}^{\text{bulk}}$ and $E_{\text{sup}}^{\text{bulk}}$ are the energies of a substrate and surface atom in the respective fcc bulk crystals, respectively.

Our results, those obtained with other theoretical methods and those deduced from experiments, all them expressed in J/m^2, are summarized in Table 2 and shown in Fig. 6 for a better comparison. In Table 2, the values of calculated work function are also compared with experiments. Notice the very good agreement between the two series of data.

Let us first comment our surface energy results corresponding to LAPW. Regarding the difference between nsp and sp calculations, the percentages are 15.1% (Co), 4.1% (Ni), 1.2% (Pt), 14.4% (PtCo) and 9.4% (PtNi). Aldén et al. [26] obtained the same conclusion for Ni and Co. If we compare our results with the experimental data, we appreciate an excellent agreement in the case of pure Co (∼1%). For Ni and Pt the differences are greater (∼25 and 33%, respectively). It is important to mention that the most of the experimental surface energy data [25] stems from surface tension measurements in the liquid phase extrapolated to zero temperature. These data do not yield information for the

Table 2
Calculated surface energies σ in J/m^2 obtained from sp and nsp calculations. The values calculated by other theoretical methods and those coming from experiments are also shown.

Surface	Surface energy (J/m^2)							Work function (eV)
	LAPW nsp sp	TB LMTO [26]	MEAM	ECT [4]	EAM [29]	FCD [31]	Exp.	LAPW Exp.
Co(111)	2.576	2.70		2.624		2.775 (0001)	2.709 [24]	5.021
	2.187						2.55 [25]	5.21 [13]
Ni(111)	1.844	2.69	2.035 [28]	2.412	1.450	2.011	2.45 [25]	5.222
	1.769		1.606 [30]				2.240 poli [27]	5.2 [32]
Pt(111)	1.653		1.656 [28]	1.769	1.440	2.299	2.691 poli [24]	5.677
	1.673		1.710 [30]				2.475 [25]	5.93 [33]
							2.49 [27]	
PtNi(111)	2.517							5.437
	2.281							
PtCo(111)	2.642							5.393
	2.261							5.56 (0.5 mL) [13]

surface energy of a particular surface facet. In addition, in a recent work published by Zhang et al. [28] they concluded that for all metals considered in the paper (Cu, Ag, Au, Ni, Pd, Pt, Al, Pb and Rh) the lowest surface energy corresponds to the close-packed (111) plane.

Looking at Fig. 6, we can say that our results of surface energies are in general agreement with those obtained with other methods. Some theoretical surface energies derived from DFT calculations have been published in the literature [26,31]. Our results are in good agreement for Co (4.8 and 7.7% of relative percentage difference in comparison with LMTO and FCD, respectively) and Ni (9.1% in comparison with FCD) but for Pt we have a 39.1% difference in comparison with FCD result. Furthermore, the results of our calculations are also in good agreement with embedding or embedding-like techniques (i.e. MEAM and ECT) for Co (1.9%, ECT), Ni (10.3 and 12.9%, MEAM) and Pt (0.2 and 3.4%, MEAM, and 7%, ECT). However, for Ni we have a 30.8% difference in comparison with ECT result.

There are not surface energy data about the bimetallic systems Pt/Ni and Pt/Co in the literature, but in a recent work, Choi et al. [34] studied the atomic segregation and magnetization of the PtNi(001) with different surface compositions (100, 50 and 0% of Pt concentration) using the FLAPW method. In spite of the fact that the surface is not the same, these authors found that the surface energies of 100%-Pt and 100%-Ni surfaces were 0.87 and 1.44 eV, respectively. This gives a difference between them of 0.57 eV. Notwithstanding, these surfaces are not the same as our models, this last value is in very good agreement with the value of 0.512 eV, corresponding to the diference of our surface energies between Pt/Ni(111) and Ni(111). Moreover, this results indicates that the Pt surface is the most stable.

In order to attain a deeper description of the electronic structure of the bimetallic systems and make a comparison with the values published in [34], we show in Table 3, the calculated local magnetic moments (in μ_B) for the different atoms of our slab models. The atom number indicates the position of the atom in the slab: 1 (bulk), 2 (medium), 3 (interface) and 4 (surface). In the bimetallic slab the atom 4 corresponds to Pt. Firstly, notice that the magnetic moment for surface Pt(4) atom differs from that of a Pt atom in the bulk of pure Pt: 0.12, 0.15 and 0.43 μ_B, for Pt(111), Pt/Ni(111) and Pt/Co(111), respectively, in comparison with 0.01 μ_B for bulk Pt. This is a well-known property due to the presence of surface states and band narrowing. It is noticeable that the subsurface Ni atom (3) in the Pt/Ni(111) slab has the largest Ni magnetic moment (0.77 μ_B), which is enhanced by 17% with respect to that of bulk Ni (0.66 μ_B). In Ref. [34], Choi et al. found in the 100%-Pt surface the same effect with an increment of the 50% between the magnetic moment of the subsurface Ni atom (0.85 μ_B) and that of bulk Ni (0.58 μ_B). It shows the importance of band hybridization on the Ni and Pt magnetization. The same effect can be appreciated for Pt/Co(111).

The ideal *adhesion or separation energy* W_{sep} is defined as the reversible work needed to separate an interface into two free surfaces, assuming no plastic or diffusional modifications. It can be given by the difference in total energy between the interface and its isolated components:

$$W_{sep} = \frac{\left(E^{subs} + 2E^{sup}_{asubs} - E^{slab}\right)}{2} \tag{3}$$

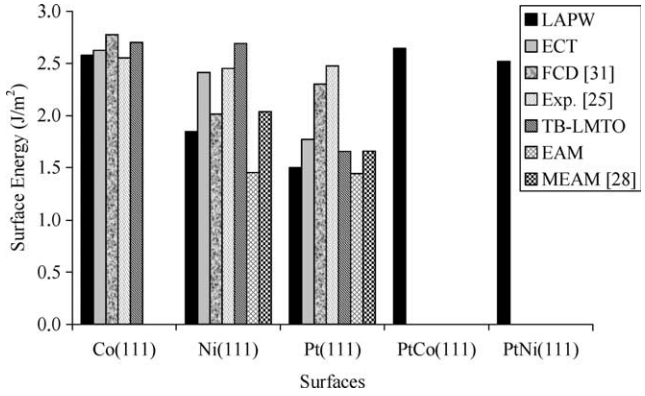

Fig. 6. Comparative graph of surface energies given in Table 2. The MEAM method and experimental data are from Refs. [28] and [25], respectively.

Table 3
Magnetic moments (in μ_B) for each no equivalent atom in the slab and for the total cell

Atom	Pt(111)	Ni(111)	Co(111)	Pt/Ni(111)	Pt/Co(111)
1	0.15161	0.65232	1.72786	0.65758	1.97400
2	0.17901	0.66026	1.72708	0.68202	1.94589
3	0.15963	0.69918	1.74634	0.76971	2.08812
4	0.11917	0.71276	1.82035	0.14711	0.42676
Cell	1.04329	4.59628	11.88852	3.72563	10.89556

The atom number indicates its position in the slab: 1 (bulk), 2 (medium), 3 (interface) and 4 (surface).

Table 4
Calculated (nsp and sp) adhesion energies

Method	Co(111)	Ni(111)	Pt(111)	PtNi(111)	PtCo(111)
LAPW nsp	1.954	1.441	1.189	0.949	1.037
LAPW sp	1.852	1.358	1.276	1.275	1.243
CASTEP nsp separation energy			1.325		1.056
CASTEP nsp adhesion energy with relaxed monolayer			0.986		0.814

All values are given in eV/at. The CASTEP method data are from Ref. [5].

where E^{subs} is the total energy of the substrate slab; E^{sup}_{asubs} is the total energy of the isolated monolayer with substrate lattice parameter and E^{slab} is the total energy of the slab. The factor 2 accounts for the presence of two surfaces in the slab.

The results obtained with Eq. (3) are summarized in Table 4. All values are given in eV/at to compare with Ref. [5]. Notice that the W_{sep} energy obtained with sp calculations is greater than that with nsp calculations. This behaviour is much more important for Pt/Ni and Pt/Co (34.3 and 12.8%, respectively) than for the case of one Pt layer deposited on Pt (7.3%). It has been theoretically demonstrated [35] and experimentally checked [3] that a surface layer under compressive stress (as our Pt/Ni and Pt/Co models) is chemically less reactive than the same surface layer under tensile stress (as our Pt/Pt model). In a previous study, a correlation was found between the adhesion energy of Pt overlayers and electronic perturbations in this metal [36]. Therefore, our present results are consistent with these references.

For Pt and Pt/Co other calculations were performed using another formalism based on DFT (the CASTEP method) [5]. The adhesion of Pt overlayer in pseudomorphic epitaxy on hcp Co(0001) was studied and compared to the adhesion of the Pt surface layer on Pt(111). The slabs were formed by one Pt layer, three substrate layers (either Co or Pt) and a vacuum gap of 10 Å. In this approach, two energies were considered: *separation energy and adhesion* energy *with relaxed monolayer*s. The first one is the energy released between two states (initial and final). For a given system, the initial state before Pt adhesion on the substrate was formed by a relaxed Pt monolayer of the proper symmetry and the infinitely separated substrate. The final state consisted of the Pt overlayer in pseudomorphic epitaxy on the substrate separated by the distance corresponding to the lowest total energy. Clearly, the Pt–Pt distance varies between the initial and final sates of the system. Then, the evolution to adhesion was decomposed in two steps. The first one is the change of the Pt–Pt distance in the free Pt monolayer (2.807 Å) to the interatomic distance in the substrate surface plane (2.62 Å). This energy checks the strain energy suffered by the Pt monolayer in the final state. In the second step, this constrained Pt monolayer is approached from infinity to the substrate (for Co, $a = 2.507$ Å). This energy released proves the strength of the Pt-substrate chemical interaction and coincides with Eq. (3).

If we now turn to Table 4 we can see a good agreement for Pt/Co (relative percentage difference: 1.8%). In the case of Pt surface the difference is 10.35%. We point out that the cell parameters employed in both methods are the same.

In Fig. 7, we compare the surface and adhesion energies (in J/m^2) obtained with LAPW, for nsp and sp cases. The trend for

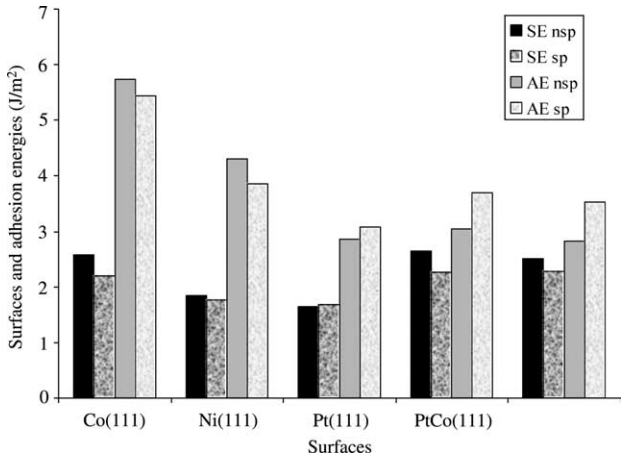

Fig. 7. Comparison between calculated surface (SE) and separation or adhesion (AE) energies in J/m^2 for nsp and sp calculations.

each surface is the same. Generally a smaller surface energy indicates a less reactive surface with a low adhesion energy and vice versa.

4. Conclusions

A GGA-DFT study of the energetic and electronic properties of the Pt, Pt/Ni and Pt/Co (111) surfaces besides Co and Ni surfaces was performed.

The electronic structure was analyzed using the concepts of the LDOS (for the Pt surface atoms). The broader d-band for the Pt overlayer in comparison with pure Pt must be outlined. The d states LDOS(E_F) is lower than on Pt(111) (1.639 for Pt, 0.875 for Pt′, 1.499 for Pt/Ni and 0.945 for Pt/Co, all these values expressed in eV^{-1}). These observations can be related to the greater overlap between the Pt atoms due to the contraction of the Pt–Pt distance in the epitaxial Pt layer, which broadens the 5d-band and depresses its general profile. This behavior is essentially due to a geometrical effect.

We have also calculated the shift in the d-band center when Pt is deposited as a pseudomorphic overlayer in comparison with Pt pure. The d-band center at the Pt surface is higher in energy than for the bulk Pt. In the bimetallic case, when a metal atom with a large lattice constant and the filling of the d-band is greater than 0.5 is put as an overlayer at the surface of a metal with a small lattice, the width of the d-band increases and therefore the local d-band to shift down in order to preserve the degree of d-band filling. The center of gravity of the d-states obtained starting from the DOS curves presented above is placed at: −2.61, -3.72 and −3.69 eV for Pt, Pt/Ni and Pt/Co, respectively, considering the nsp calculations; on the other hand, with for sp calculations the average between up and down DOS curves gives: −2.62, −3.69 and −3.71 eV, respectively.

The calculated surface energies (σ) for pure surfaces are in agreement with the general experimental evidences and with the other theoretical results, in particular for Co. The trend is: $\sigma(\text{Pt/Co}) > \sigma(\text{Co}) > \sigma(\text{Pt/Ni}) > \sigma(\text{Ni}) > \sigma(\text{Pt})$.

The magnetism in the bimetallic systems was also studied by calculating the magnetic moments for all these surfaces. We notice that the subsurface atom in the different slabs has a magnetic moment which is enhanced from that of the respective bulk.

Finally, the calculated separation energies (W_{sep}) for Co, Ni, Pt, Pt/Co and Pt/Ni were considered. For the bimetallic systems the W_{sep} obtained with sp calculations is much greater than that with nsp calculations, in comparison with pure platinum. On the other hand, if we compare the surface and separation energies (in J/m^2) obtained with LAPW, with nsp and sp calculations, the trend for each surface is the same. Generally a smaller surface energy indicates a less reactive surface with a low adhesion energy and vice-versa.

Acknowledgements

G.F.C. and N.J.C. are indebted to CONICET and Departamento de Física of UNS, Argentina, for financial support.

References

[1] J.A. Rodriguez, D.W. Goodman, Science 257 (1992) 897.
[2] G.F. Cabeza, N.J. Castellani, P. Légaré, Surf. Rev. Lett. 6 (3–4) (1999) 369.
[3] G.F. Cabeza, P. Légaré, N.J. Castellani, Surf. Sci. 465 (2000) 286–300.
[4] P. Legaré, G.F. Cabeza, N.J. Castellani, Surf. Rev. Lett. 5 (1998) 581.
[5] P. Legaré, N.J. Castellani, G.F. Cabeza, Surf. Sci. 496 (2000) L51–L54.
[6] E. Bauer, J.H. Van der Merwe, Structure and growth of crystalline superlattices: from monolayer to superlattice, Phys. Rev. B 33 (1986) 3657.
[7] C. Argile, G.E. Rhead, Adsorbed layer and thin film growth modes monitored by Auger electron spectroscopy, Surf. Sci. Rep. 10 (1989) 277.
[8] J.A. Barnard, J.J. Ehrhardt, J. Vac. Sci. Technol. A 8 (1990) 4061; S. Deckers, S. Offerhaus, W.F. Van der Weg, F.H.P.M. Habraken, Surf. Sci. 237 (1990) 203.
[9] S. Deckers, F.H.P.M. Habraken, W.F. van der Weg, J.W. Geus, Appl. Surf. Sci. 45 (1990) 207.
[10] A. Barbier, PhD thesis, Université Louis Pasteur, Strasbourg, 1993.
[11] H. Bulou, A. Barbier, R. Belkhou, C. Guillot, B. Carrière, J. Deville, Surf. Sci. 352–354 (1996) 26.
[12] J.P. Perdew, S. Burke, M. Ernzerhof, Phys. Rev. Lett. 77 (1996) 3865.
[13] G.F. Cabeza, P. Légaré, N.J. Castellani, Surf. Sci. 457 (2000) l21–l33.
[14] Ch. Lu, I. Lee, R.I. Masel, A. Wieckowski, C. Rice, J. Phys. Chem. A 106 (2002) 3084.
[15] B. Hammer, J.K. Nørskov, Surf. Sci. 343 (1995) 211; B. Hammer, J.K. Nørskov, Adv. Catal. 45 (2000) 71.
[16] B. Hammer, O.H. Nielsen, J.K. Nørskov, Catal. Lett. 46 (1997) 31.
[17] P. Légaré, G.F. Cabeza, N.J. Castellani, Catal. Today 89 (3) (2004) 363.
[18] A. Ruban, B. Hammer, P. Stoltze, H.L. Skriver, J.K. Nørskov, J. Mol. Catal. A Chem. 115 (1997) 421.
[19] G.F. Cabeza, N.J. Castellani, P. Légaré, Comput. Mater. Sci. 17 (2–4) (2000) 255.
[20] P. Legaré, B. Madani, G.F. Cabeza, N.J. Castellani, Int. J. Mol. Sci. 2 (5) (2001) 246.
[21] S. Pick, Surf. Sci. 352–354 (1996) 300.
[22] J.A. Rodriguez, Surf. Sci. Rep. 24 (1996) 223–287.
[23] J.J. Metóis, P. Müller, Surf. Sci. 548 (2004) 13–21.
[24] L.Z. Mezey, J. Giber, Jpn. J. Appl. Phys. 21 (1982) 1569.
[25] F.R. De Boer, R. Boom, W.C.M. Mattens, A.R. Miedema, A.K. Niessen, in: F.R. De Boer, D.G. Pettifor (Eds.), Cohesion in Metals vol. 1 (1988), p. 676.
[26] M. Aldén, S. Mirbt, H.L. Skriver, N.M. Rosengaard, B. Johansson, Phys. Rev. B 46 (10) (1992) 6303.
[27] W.R. Tyson, W.A. Miller, Surf. Sci. 62 (1977) 267.
[28] J.-M. Zhang, F. Ma, K.-W. Xu, Appl. Surf. Sci. 229 (2004) 34.
[29] S.M. Foiles, M.I. Baskes, M.S. Daw, Phys. Rev. B 33 (12) (1986) 7983.
[30] B.-J. Lee, J.-H. Shim, M.I. Baskes, Phys. Rev. B 68 (2003) 44112.
[31] L. Vitos, A.V. Ruban, H.L. Skriver, J. Kollár, Surf. Sci. 411 (1998) 186.
[32] V.S. Fomenko, I.A. Podtshemaijeva, Emissionnyje I Adsorbtionnyje Svojstva Materialov, Atomizdat, Moscow, 1975.
[33] D.R. Lide, CRC Handbook of Chemistry and Physics, 80th ed., CRC Press, New York, 1999.
[34] S.Y. Choi, Y.S. Kwon, S.C. Hong, J.I. Lee, R.Q. Wu, J. Magn. Magn. Mater. 226–230 (2001) 1662.
[35] M. Mavrikakis, B. Hammer, J.K. Nørskov, Phys. Rev. Lett. 81 (1998) 2819.
[36] J.A. Rodriguez, Surf. Sci. 345 (1996) 347–362.